Extruded tellurite glass and fibers with low OH content for mid-infrared applications

Heike Ebendorff-Heidepriem,* Kevin Kuan, Michael R. Oermann, Kenton Knight, and Tanya M. Monro

Institute of Photonics & Advanced Sensing, School of Chemistry & Physics, The University of Adelaide, Adelaide, SA5005, Australia
**heike.ebendorff@adelaide.edu.au*

Abstract: Reducing the hydroxyl group content in tellurite glass fibers is essential to exploit the intrinsic mid-infrared transparency of tellurite glass for optical fiber devices. We report the first extruded tellurite glass fibers with low hydroxyl (OH) group content using dry atmosphere for glass melting. For small melt volumes, optimized melting conditions have been identified that enable the absorption at the OH peak at 3.3 µm to be reduced by more than an order of magnitude compared with glasses melted in open air. Annealing and dehydration of tellurite glass in open air was found not to change the OH content. The loss of optical fibers drawn from extruded rods was reduced from ~20 dB/m at 2.0 µm for glass melted in open air to 0.8 dB/m for glass melted in dry atmosphere.

OCIS codes: (160.2290) Fiber materials; (160.2750) Glass and other amorphous materials; (060.2390) Fiber optics, infrared.

References and links

1. G. Qin, M. Liao, C. Chaudhari, X. Yan, C. Kito, T. Suzuki, and Y. Ohishi, "Second and third harmonics and flattened supercontinuum generation in tellurite microstructured fibers," Opt. Lett. **35**(1), 58–60 (2010), http://www.opticsinfobase.org/abstract.cfm?URI=ol-35-1-58.
2. G. Qin, X. Yan, C. Kito, M. Liao, T. Suzuki, A. Mori, and Y. Ohishi, "Zero-dispersion-wavelength-decreasing tellurite microstructured fiber for wide and flattened supercontinuum generation," Opt. Lett. **35**(2), 136–138 (2010), http://www.opticsinfobase.org/abstract.cfm?URI=ol-35-2-136.
3. G. Qin, X. Yan, C. Kito, M. Liao, T. Suzuki, A. Mori, and Y. Ohishi, "Highly nonlinear tellurite microstructured fibers for broadband wavelength conversion and flattened supercontinuum generation," J. Appl. Phys. **107**(4), 043108 (2010).
4. M. Liao, C. Chaudhari, G. Qin, X. Yan, T. Suzuki, and Y. Ohishi, "Tellurite microstructure fibers with small hexagonal core for supercontinuum generation," Opt. Express **17**(14), 12174–12182 (2009), http://www.opticsinfobase.org/abstract.cfm?URI=oe-17-14-12174.
5. M. Liao, X. Yan, G. Qin, C. Chaudhari, T. Suzuki, and Y. Ohishi, "A highly non-linear tellurite microstructure fiber with multi-ring holes for supercontinuum generation," Opt. Express **17**(18), 15481–15490 (2009), http://www.opticsinfobase.org/abstract.cfm?URI=oe-17-18-15481.
6. P. Domachuk, N. A. Wolchover, M. Cronin-Golomb, A. Wang, A. K. George, C. M. B. Cordeiro, J. C. Knight, and F. G. Omenetto, "Over 4000 nm bandwidth of mid-IR supercontinuum generation in sub-centimeter segments of highly nonlinear tellurite PCFs," Opt. Express **16**(10), 7161–7168 (2008), http://www.opticsinfobase.org/abstract.cfm?URI=oe-16-10-7161.
7. X. Feng, W. H. Loh, J. C. Flanagan, A. Camerlingo, S. Dasgupta, P. Petropoulos, P. Horak, K. E. Frampton, N. M. White, J. H. V. Price, H. N. Rutt, and D. J. Richardson, "Single-mode tellurite glass holey fiber with extremely large mode area for infrared nonlinear applications," Opt. Express **16**(18), 13651–13656 (2008), http://www.opticsinfobase.org/abstract.cfm?URI=oe-16-18-13651.
8. D. Buccoliero, H. Steffensen, H. Ebendorff-Heidepriem, T. M. Monro, and O. Bang, "Midinfrared optical rogue waves in soft glass photonic crystal fiber," Opt. Express **19**(19), 17973–17978 (2011), http://www.opticsinfobase.org/abstract.cfm?URI=oe-19-19-17973.
9. D. Buccoliero, H. Steffensen, O. Bang, H. Ebendorff-Heidepriem, and T. M. Monro, "Thulium pumped high power supercontinuum in loss-determined optimum lengths of tellurite photonic crystal fiber," Appl. Phys. Lett. **97**(6), 061106 (2010).
10. G. Qin, A. Mori, and Y. Ohishi, "Brillouin lasing in a single-mode tellurite fiber," Opt. Lett. **32**(15), 2179–2181 (2007), http://www.opticsinfobase.org/abstract.cfm?URI=ol-32-15-2179.
11. G. Qin, R. Jose, and Y. Ohishi, "Design of ultimate gain-flattened O-, E-, and S+ C+ L ultrabroadband fiber amplifiers using a new fiber Raman gain medium," J. Lightwave Technol. **25**(9), 2727–2738 (2007).

#162011 - $15.00 USD Received 23 Jan 2012; revised 1 Mar 2012; accepted 8 Mar 2012; published 16 Mar 2012

12. G. Qin, M. Liao, T. Suzuki, A. Mori, and Y. Ohishi, "Widely tunable ring-cavity tellurite fiber Raman laser," Opt. Lett. **33**(17), 2014–2016 (2008), http://www.opticsinfobase.org/abstract.cfm?URI=ol-33-17-2014.
13. A. Mori, H. Masuda, K. Shikano, and M. Shimizu, "Ultra-wide-band tellurite-based fiber Raman amplifier," J. Lightwave Technol. **21**(5), 1300–1306 (2003).
14. J. Dong, Y. Q. Wei, A. Wonfor, R. V. Penty, I. H. White, J. Lousteau, G. Jose, and A. Jha, "Dual-pumped tellurite fiber amplifier and tunable. laser using Er /Ce codoping scheme," IEEE Photon. Technol. Lett. **23**(11), 736–738 (2011).
15. F. Fusari, A. A. Lagatsky, G. Jose, S. Calvez, A. Jha, M. D. Dawson, J. A. Gupta, W. Sibbett, and C. T. A. Brown, "Femtosecond mode-locked Tm^{3+} and Tm^{3+}-Ho^{3+} doped 2 μm glass lasers," Opt. Express **18**(21), 22090–22098 (2010), http://www.opticsinfobase.org/abstract.cfm?URI=oe-18-21-22090.
16. K. Li, G. Zhang, and L. Hu, "Watt-level ~2 μm laser output in Tm^{3+}-doped tungsten tellurite glass double-cladding fiber," Opt. Lett. **35**(24), 4136–4138 (2010), http://www.opticsinfobase.org/abstract.cfm?URI=ol-35-24-4136.
17. Y. Tsang, B. Richards, D. Binks, J. Lousteau, and A. Jha, "A Yb^{3+}/Tm^{3+}/Ho^{3+} triply-doped tellurite fibre laser," Opt. Express **16**(14), 10690–10695 (2008), http://www.opticsinfobase.org/abstract.cfm?URI=oe-16-14-10690.
18. B. Richards, Y. Tsang, D. Binks, J. Lousteau, and A. Jha, "Efficient ~2 μm Tm^{3+}-doped tellurite fiber laser," Opt. Lett. **33**(4), 402–404 (2008), http://www.opticsinfobase.org/abstract.cfm?URI=ol-33-4-402.
19. A. Mori, K. Kobayashi, M. Yamada, T. Kanamori, K. Oikawa, Y. Nishida, and Y. Ohishi, "Low noise broadband tellurite-based Er^{3+}-doped fibre amplifiers," Electron. Lett. **34**(9), 887–888 (1998).
20. T. M. Monro and H. Ebendorff-Heidepriem, "Progress in microstructured optical fibers," Annu. Rev. Mater. Res. **36**(1), 467–495 (2006).
21. K. Richardson, D. Krol, and K. Hirao, "Glasses for photonic applications," Int. J. Appl. Glass. Sci. **1**(1), 74–86 (2010).
22. J. S. Wang, E. M. Vogel, and E. Snitzer, "Tellurite glass: new candidate for fiber devices," Opt. Mater. **3**(3), 187–203 (1994).
23. M. R. Oermann, H. Ebendorff-Heidepriem, Y. Li, T.-C. Foo, and T. M. Monro, "Index matching between passive and active tellurite glasses for use in microstructured fiber lasers: erbium doped lanthanum-tellurite glass," Opt. Express **17**(18), 15578–15584 (2009), http://www.opticsinfobase.org/abstract.cfm?URI=oe-17-18-15578.
24. A. Lin, A. Ryasnyanskiy, and J. Toulouse, "Fabrication and characterization of a water-free mid-infrared fluorotellurite glass," Opt. Lett. **36**(5), 740–742 (2011), http://www.opticsinfobase.org/abstract.cfm?URI=ol-36-5-740.
25. G. Liao, Q. Chen, J. Xing, H. Gebavi, D. Milanese, M. Fokine, and M. Ferraris, "Preparation and characterization of new fluorotellurite glasses for photonics application," J. Non-Cryst. Solids **355**(7), 447–452 (2009).
26. M. D. O'Donnell, C. A. Miller, D. Furniss, V. K. Tikhomirov, and A. B. Seddon, "Fluorotellurite glasses with improved mid-infrared transmission," J. Non-Cryst. Solids **331**(1-3), 48–57 (2003).
27. J. Massera, A. Haldeman, J. Jackson, C. Rivero-Baleine, L. Petit, and K. Richardson, "Processing of tellurite-based glass with low OH content," J. Am. Ceram. Soc. **94**(1), 130–136 (2011).
28. A. Mori, "Tellurite-based fibers and their applications to optical communication networks," J. Ceram. Soc. Jpn. **116**(1358), 1040–1051 (2008).
29. H. Gebavi, D. Milanese, G. Liao, Q. Chen, M. Ferraris, M. Ivanda, O. Gamulin, and S. Taccheo, "Spectroscopic investigation and optical characterization of novel highly thulium doped tellurite glasses," J. Non-Cryst. Solids **355**(9), 548–555 (2009).
30. A. Lin, A. Zhang, E. J. Bushong, and J. Toulouse, "Solid-core tellurite glass fiber for infrared and nonlinear applications," Opt. Express **17**(19), 16716–16721 (2009), http://www.opticsinfobase.org/abstract.cfm?URI=oe-17-19-16716.
31. X. Feng, S. Tanabe, and T. Hanada, "Hydroxyl groups in erbium-doped germane-tellurite glasses," J. Non-Cryst. Solids **281**(1-3), 48–54 (2001).
32. A. N. Moiseev, V. V. Dorofeev, A. V. Chilyasov, I. A. Kraev, M. F. Churbanov, T. V. Kotereva, V. G. Pimenov, G. E. Snopatin, A. A. Pushkin, V. V. Gerasimenko, A. F. Kosolapov, V. G. Plotnichenko, and E. M. Dianov, "Production and properties of high purity TeO_2–ZnO–Na_2O–$Bi_2O_3$and TeO_2–WO_3–La_2O_3–MoO_3 glasses," Opt. Mater. **33**(12), 1858–1861 (2011).
33. M. F. Churbanov, A. N. Moiseev, A. V. Chilyasov, V. V. Dorofeev, I. A. Kraev, M. M. Lipatova, T. V. Kotereva, E. M. Dianov, V. G. Plotnichenko, and E. B. Kryukova, "Production of high-purity TeO_2-ZnO and TeO_2-WO_3 glasses with reduced content of OH groups," J. Optoelectron. Adv. Mater. **9**, 3229–3234 (2007).
34. M. R. Oermann, H. Ebendorff-Heidepriem, D. J. Ottaway, D. G. Lancaster, P. J. Veitch, and T. M. Monro, "Extruded microstructured tellurite fibre lasers," IEEE Photon. Technol. Lett. (to be published).
35. H. Ebendorff-Heidepriem, R. C. Moore, and T. M. Monro, "Progress in the fabrication of the next-generation soft glass microstructured optical fibers," in *Proc. 1st International Workshop on Speciality Optical Fibers*, Sao Pedro, Brazil, Aug 2008.
36. H. Ebendorff-Heidepriem and T. M. Monro, "Extrusion of complex preforms for microstructured optical fibers," Opt. Express **15**(23), 15086–15092 (2007), http://www.opticsinfobase.org/abstract.cfm?URI=oe-15-23-15086.
37. H. Ebendorff-Heidepriem and D. Ehrt, "Determination of the OH content of glasses," Glastech. Ber. **68**, 139146 (1995).
38. S. Blanchandin, P. Marchet, P. Thomas, J. C. Champarnaud-Mesjard, B. Frit, and A. Chagraoui, "New investigations within the TeO_2-WO_3 system: phase equilibrium diagram and glass crystallization," J. Mater. Sci. **34**(17), 4285–4292 (1999).
39. E. V. Zorin, M. F. Churbanov, G. E. Snopatin, I. A. Grishin, T. A. Petrova, and V. G. Plotnichenko, "Microinhomogeneities in tellurite glasses," Inorg. Mater. **41**(7), 775–778 (2005).

#162011 - $15.00 USD Received 23 Jan 2012; revised 1 Mar 2012; accepted 8 Mar 2012; published 16 Mar 2012

40. C. A. Click, R. K. Brow, P. R. Ehrmann, and J. H. Campbell, "Characterization of Pt^{4+} in alumino-metaphosphate laser glasses," J. Non-Cryst. Solids **319**(1-2), 95–108 (2003).

1. Introduction

Tellurite glasses have been demonstrated to be attractive materials for high nonlinearity fibers and rare earth doped fiber lasers and amplifiers [1–19]. This stems from the fact that they have unique properties that set them apart from other oxide glasses such as silicates, borates and phosphates. Of all oxide glasses, tellurite glasses exhibit the widest transmission range of 0.3-4 μm [20,21]. The mid-infrared transmission at 2-4 μm is of particular interest, as this cannot be achieved with silica, which is the most widely used fiber material. Compared with other mid-infrared transmitting glasses such as fluorides and chalcogenides, tellurite glasses demonstrate higher corrosion, crystallization and thermal stability [22]. In addition, they are non-hygroscopic, which allows storage in ambient air without degradation. Of all oxide glasses, tellurite glasses exhibit the highest linear and nonlinear refractive indices [20,21], which has attracted growing interest for supercontinuum generation [1–9] and Raman lasers [12–14]. Tellurite glasses also show advantages as host materials for rare earth laser ions [14–19,23]. High concentrations of rare earth ions can be incorporated in tellurite glass without clustering, rare earth ions show broad emission bands in tellurite glass, and tellurite glasses also exhibit the lowest phonon energy among oxide glasses [20–22].

In recent years, the use of tellurite glass fibers for supercontinuum generation and lasing in the mid-infrared >2 μm has attracted particular interest, as this cannot be achieved with silica fibers. However, the exploitation of tellurite glass in the mid-infrared is hampered by the fact that tellurite glasses exhibit high water content when melted in ambient atmosphere. Water in the raw materials or atmosphere is incorporated into the glass as hydroxyl (OH) groups that show broad and intense absorption at 3-4 μm with peak at 3.3 μm [24–33]. Several methods have been investigated to fabricate tellurite glasses with low OH content. One effective method is to use fluorides in the glass batch, i.e. to fabricate fluorotellurite glasses [24–27]. However, this changes significantly the glass properties, making them more similar to those of fluoride glasses [24], which does not fully exploit the advantageous properties that tellurite glass offers compared to fluoride glass. In particular, the decrease in glass transition temperature and linear and nonlinear refractive index [24] is undesired for high gain lasers and nonlinear devices. Other techniques include melting in dry atmosphere or bubbling of reactive gases through the melt [27–33]. Purification of raw materials and drying of raw material batches in vacuum have also been reported [28,30,32,33]. For fluoride-free tellurite glasses, the use of ultrahigh-purity raw materials combined with melting in dry atmosphere resulted in glasses in which the absorption due to OH groups was reduced to a few dB/m at 3.3 μm (corresponding to an absorption coefficient of ~0.001 cm^{-1}) [32,33]. Using such purified tellurite glasses, multimode polymer-clad fibers made using cast preforms or using the crucible method demonstrated losses of 0.2-0.4 dB/m at 1.5-2.0 μm [32]. The lowest loss achieved for a multimode tellurite fiber with tellurite glass cladding is 0.02 dB/m at 1.56 μm [13,28]. This fiber was made using the casting technique for the core/clad preform fabrication and ultrahigh-purity TeO_2 raw material for glass fabrication. However, such ultra-high purity raw materials are not commercially available and raw material purification is resource-intensive, which limits the development of optical tellurite fibers with tailored fiber design and low OH content.

In this paper, we report the first extruded tellurite glass fibers with low OH content. Using commercial raw materials, we explored dehydration of tellurite glass and fabrication of optical fibers using the tellurite glasses with low OH content. We used the extrusion technique for preform fabrication as this technique has been demonstrated to be a viable method for the manufacture of microstructured tellurite fibers that show great promise for lasing [34] and supercontinuum generation [1–4,8,9,28]. For the investigations, we selected the known glass composition 73 TeO_2 – 20 ZnO – 5 Na_2O – 2 La_2O_3 (in mol%) that was found to be an attractive glass for rare earth doped fiber lasers [23] and nonlinear devices including supercontinuum generation [8,9], and which can be extruded into a variety of preform

#162011 - $15.00 USD Received 23 Jan 2012; revised 1 Mar 2012; accepted 8 Mar 2012; published 16 Mar 2012

structures [34,35]. We investigated the impact of melting time, melt volume and swirling on the OH content of the fabricated glass. In addition, we explored effect of preform extrusion and fiber drawing on the OH content. Furthermore, the correlation between the loss at the OH peak at 3.3 μm in the glass and the infrared loss (up to 2.4 μm) of the corresponding fibers was studied.

2. Experimental approach

The properties of the selected glass composition (73 TeO_2 – 20 ZnO – 5 Na_2O – 2 La_2O_3 in mol%) when melted in ambient atmosphere are reported in [23]. The glass samples were prepared using 30-100 g batch weight. The commercially available raw materials (Alfa Aesar, Sigma-Aldrich, International Laboratory, Suzhou Sinosun) used were TeO_2, ZnO, Na_2CO_3 and La_2O_3 with 99.99% or higher purity. The majority of the glasses reported here were melted in gold crucibles. A few melts were also performed within platinum crucibles. All glasses were melted at 850-900 °C, cast into preheated brass moulds and annealed at 315 °C. The glasses were batched, swirled, cast and annealed in a glovebox purged with dry nitrogen (≤10 ppmv water). The glasses were melted within a silica liner that was located inside a tube furnace (hereafter referred to as melting furnace). The melting furnace liner was attached to the glovebox in a gas-tight configuration, and was (independently of the glovebox) purged with 4 L/min of a gas mixture with similar composition to air, i.e. 80% nitrogen (99.99% purity) and 20% oxygen (99.9% purity). Both gases were dried using a molecular sieve before entering the melting furnace liner. The water content of the thus dried gas mixture was measured to be 10 ppmv. This dry gas mixture is hereafter referred to as 'dry air', and hence the glasses melted in dry air and the corresponding rods and fibers made from these glasses are hereafter referred to as 'dry air' samples. For swirling and casting, the crucible with the glass melt was moved from the melting furnace liner into the glovebox.

For comparison, we also prepared glasses (made from the same raw materials) that were melted, cast and annealed in ambient atmosphere. These glasses and corresponding rods and fibers are hereafter referred to as 'open air' samples. We fabricated two different types of glass samples: rectangular glass blocks of dimensions 15x10x30 mm^3 for spectroscopic measurements and cylindrical glass billets of 30 mm diameter and 20 mm height for fiber fabrication.

To fabricate unstructured fibers from these cylindrical billets, we first extruded the glass billets into 10 mm diameter rods using the billet extrusion technique [36]. The billets were extruded through stainless steel dies at 354 °C with a speed of 0.2 mm/min. The extrusion body and the space beneath the extrusion die were purged with nitrogen (99.99% purity, 50 ppmv water). The rods were annealed at 315°C in ambient atmosphere and drawn down to unclad fibers of 160 μm outer diameter using a fiber drawing tower. The tower furnace body was purged with nitrogen or a mixture of 70% nitrogen and 30% oxygen, which had the same purity as the gases used for glass melting.

To evaluate the OH content of the glasses and extruded performs, we measured the transmission spectra in the mid-infrared at 2-6 μm, where OH groups show strong absorption. For measurements of the transmission spectra, polished glass samples of 2-20 mm thickness were prepared from the glass blocks, billets and extruded glass rods. The samples were polished using aqueous ceria slurry and stored in ambient atmosphere. Transmission spectra in the wavelength range of 2-10 μm were measured using commercial FTIR spectrometer (PerkinElmer FTIR 400). Background absorbance due to Fresnel reflection and sample surface imperfection were subtracted from the measured spectra prior to calculation of the attenuation loss. The measurement error is ± 5 dB/m.

To evaluate the impact of OH content and choice of crucible material on the attenuation of the fibers made, we measured fiber loss spectra using the cutback technique and commercial optical spectrum analyzers (OSAs) ranging from 400 to 1700 nm and 1200-2400 nm. We used two different white light sources – a tungsten filament bulb together with the 400-1700 nm OSA and a supercontinnuum source (KOHERAS SuperK™ Compact) together with the 1200-2400 nm OSA. The supercontinuum light source resulted in larger noise. For each fiber,

#162011 - $15.00 USD Received 23 Jan 2012; revised 1 Mar 2012; accepted 8 Mar 2012; published 16 Mar 2012

cutback lengths of ~2 m were used. The number of cutbacks required depended on the fiber loss. We performed 3 cleaves for each cutback length to ensure that cleave variability did not impact the results. The fiber output was coupled to the OSA using a bare fiber adaptor. The measurement error is 10%.

3. Impact of glass melting conditions

Using 30-50 g batches, we explored the impact of two different 'dry air' melting methods.

(i) 900 °C melting temperature and using a crucible lid

(ii) 850 °C melting temperature without using a crucible lid.

Method (i) resembles the melting procedure we have been using for 'open air' glasses, where 900 °C melting temperature, a crucible lid and manual swirling for melt homogenization is employed. For swirling the melt, the crucible was taken out of the furnace, the lid was removed, the crucible was swirled manually for approximately 5-10 s and finally the crucible with lid was placed back into the furnace. For method (ii), the crucible lid was removed 5-10 min after the furnace reached the melting temperature of 850 °C. As no crucible lid was used, we used a lower melting temperature compared to method (i) to minimize possible evaporation during melting.

The mid-infrared absorption spectra of the thus made glasses are shown in Fig. 1(a). For comparison, the spectrum of a glass melted in open air is also shown. The spectra are composed of two OH bands at 3.3 μm and 4.4 μm. In addition, there is a shoulder in the spectrum at 3.0 μm. The shape of this spectrum is similar to that found for 10 Na_2O – 10 ZnO – 80 TeO_2 glass [26]. For this glass, deconvolution of the band at 3.3 μm demonstrated that it is composed of a narrow, lower-intensity band at 3.0 μm, which was ascribed to free OH groups, and a broad, high-intensity band at 3.3 μm due to weakly hydrogen bonded OH groups. The band at 4.4 μm was attributed to strongly hydrogen bonded OH groups [26]. As the extinction coefficient for OH absorption in tellurite glass is unknown, we used here the peak loss value of the most pronounced OH band at 3.3 μm as a relative measure of the OH content in the glasses [37]. Another reason for investigating the OH loss and not the absolute OH content is that for the use of the glasses and fibers in the mid-infrared applications the loss caused by OH impurities determines the suitability of a glass or fiber for mid-infrared applications. In Fig. 1(b), the peak loss values are plotted as a function of melting time and number of times the melt was swirled.

#162011 - $15.00 USD Received 23 Jan 2012; revised 1 Mar 2012; accepted 8 Mar 2012; published 16 Mar 2012

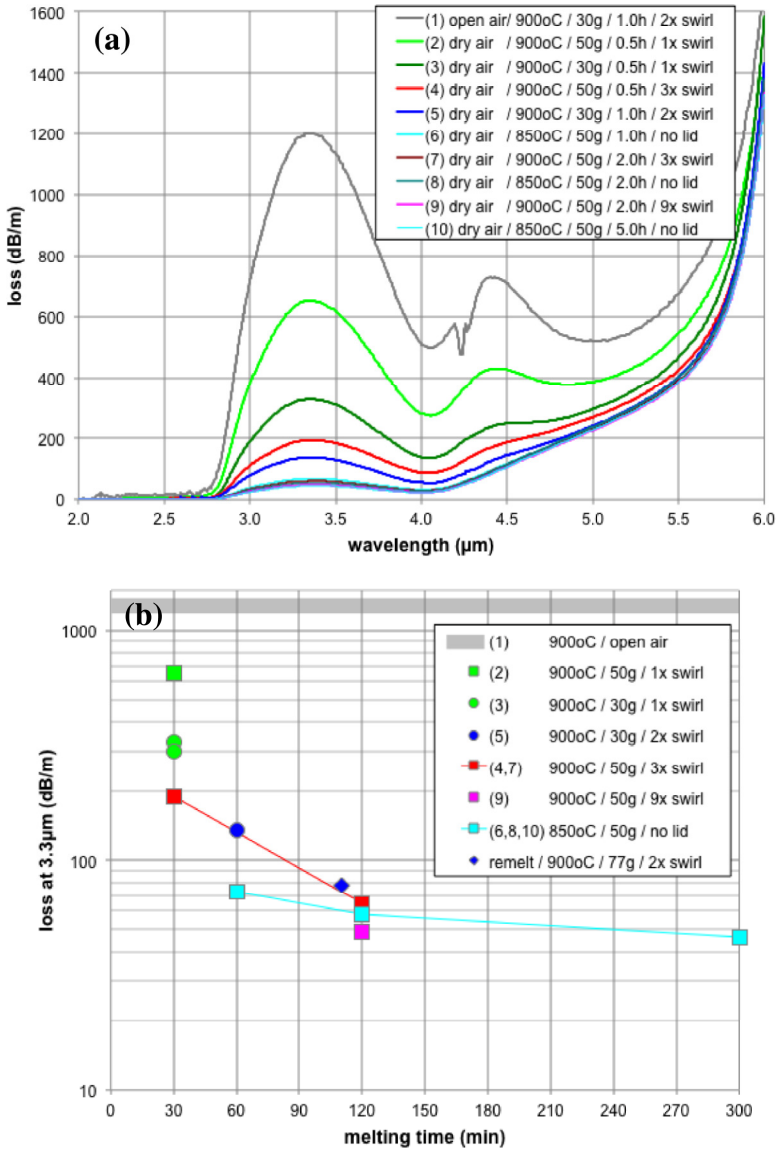

Fig. 1. (a) Loss spectra of glass samples (1-10) made from 30 to 50 g batch melts using different fabrication conditions as detailed in the legend. (b) Loss of the OH absorption at 3.3 µm as a function of melting time for 30-50 g batch melts (samples 1-10). The grey region at 1200-1400 dB/m designates the loss of 'open air' glasses. The ◆ data point refers to the sample made via remelting of an 'open air' glass in dry air.

Figure 1 demonstrates that the OH content strongly decreases with melting time and number of times the melt was swirled. For short melting time of 30 min, using a crucible lid and only swirling the melt once, the OH content of the 50 g batch melt (sample 2) was only reduced to ~600 dB/m, a reduction by approximately a factor of 2 relative to 'open air' glasses. Use of a smaller batch weight of 30 g (and thus larger surface-to-volume ratio) led to a larger reduction in OH content (down to ~300 dB/m for sample 3). Longer melting time of 60 min and/or removal of the lid or larger numbers of melt swirling significantly reduced the OH content to 200-70 dB/m (samples 4-6). A further increase in the melting time and/or number of times the melt was swirled was found to lead to only a slight additional reduction of the OH content (samples 7-10), with losses at the OH absorption peak of 60-40 dB/m for

#162011 - $15.00 USD Received 23 Jan 2012; revised 1 Mar 2012; accepted 8 Mar 2012; published 16 Mar 2012

such samples. Using similar melting time, number of melt swirling and melt volume, we observed that the remelting of an 'open air' glass in dry air led to a similar OH content compared with melting of a batch in dry air (Fig. 1(b)).

As all raw materials were handled and batched in dry atmosphere, the relatively high OH content that is observed when short melting times are used in dry air implies that the raw materials contain a significant amount of water, which becomes incorporated into the glass network during melting. Using the average extinction coefficient of 70 L/mol/cm for silica [37] and the density of our tellurite glass (5.35 g/cm^3), the OH peak loss value of 1200 dB/m of the 'open air' glass corresponds to ~30 ppm (weight) water in the glass. We assume this amount of water to stem from the commercial raw materials. As described above, when an 'open air' glass is remelted in 'dry air', this remelted 'dry air' glass exhibits a similar OH content as the corresponding batch-melted 'dry air' glass (sample 7). This result indicates that the batch and the 'open air' glass contain similar OH content, which supports the assumption that the OH content in 'open air' glass mainly originates from the water in the raw materials batch.

The OH groups in the glass melt can react with each other and form water molecules that can be released from the melt. Vice versa, water vapor in the atmosphere can react with the glass melt and form OH groups. According to this reversible reaction, the OH content in the melt can be reduced via decreasing the amount of water vapor above the glass melt. Churbanov et al. [33] demonstrated that the OH content in a tungsten-tellurite glass decreased as the water pressure over the glass melt was reduced. For our experimental conditions, when melting in open air, the moisture content in the air hinders the removal of water from the glass melt. When melting in flowing dry gas, the absence of water in the atmosphere above the glass melt forces the water out of the glass melt with increasing melting time until a steady-state is achieved. This process will become faster when the released water can be more efficiently removed from the atmosphere above the glass melt. For melts performed without lid, the water that evaporates from the melt is readily conducted away by the constant flow of dry gas. For the melts performed with a lid on the crucible, each time the melt is swirled (i.e. when the crucible is taken out of the furnace and the crucible lid is removed for the time the melt is swirled), the moisture above the melt is removed. Thus the more often the melt is swirled, the more water can be removed. In addition, larger surface-to-volume ratio of a glass melt facilitates water removal. Despite larger batch weight (and thus smaller surface-to-volume ratio), the 77 g remelt shows similar (and not significantly higher) OH content compared with the corresponding 50 g batch melt (sample 7). For the remelt, shortly after the crucible with the glass is placed in the furnace, the glass is already fully molten, whereas for a batch melt approximately 10-20 min are required to completely melt all raw materials and form a homogeneous liquid. The shorter time to form the glass liquid in case of the remelt would result in an effectively longer time available for dehydration, which would counterbalance the larger melt volume.

For our melting conditions using dry gas flow of 4 L/min and 30-50 g batch in a 100 mL crucible, the lowest water content that can be achieved is 40-50 dB/m. Further water removal is expected to require the use of higher gas flow rates or a vacuum or drier gas.

As not only water but also glass constituents can evaporate from the melt, efficient water removal may be accompanied by larger glass melt evaporation and hence possible change in glass composition. In our case, the maximum evaporation is 2.0 wt% for 5 h melting time at 850 °C without lid. Of all glass components, TeO_2 has the lowest melting point and thus is assumed to be preferentially evaporated. However, as TeO_2 is the main component (82 wt%), preferential evaporation of 2 wt% TeO_2 is expected not to change significantly the glass composition, which agrees with the fact that the density variation between glasses melted with or without lid is the measurement error of ± 0.02 g/cm^3.

#162011 - $15.00 USD Received 23 Jan 2012; revised 1 Mar 2012; accepted 8 Mar 2012; published 16 Mar 2012

4. Fabrication and characterization of optical fibers made from 'open air' and 'dry air' tellurite glass

The fibers were fabricated using glass billets made from 100 g batch weight. The fibers reported here are listed in Table 1 and their loss spectra are shown in Fig. 2. The loss spectra, in particular for the 'open air' fibers, demonstrate a distinct peak at 1.48 µm. This peak is attributed to the overtone of the vibration of free OH groups at 3.0 µm.

Table 1. Fabrication Conditions and Properties of Fibers Made

Billet Rod Fibre No.	TeO_2 purity (%)	crucible material	melting atmosphere	billet: loss (dB/m) of OH peak at 3.3µm	rod: loss (dB/m) of OH peak at 3.3µm	fiber: loss (dB/m) of OH peak at 1.5µm	fiber: minimum loss (dB/m)
#1	99.99	Au	open air	n/m	n/m	1.02	0.26
#2	99.99	Pt	open air	n/m	n/m	1.08	0.50
#3	99.999	Au	open air	n/m	1400	0.90	0.05
#4[a]	99.999	Au	dry air	90	90	0.31	0.28
#5[b]	99.999	Pt	dry air	n/m	250	0.22	0.10
#6[c]	99.999	Pt	dry air	100	100	1.41	1.27

[a]crack in rod
[b]lower meting temperature of 700-800°C for 1h
[c]bubbles in rod due to crack in billet
n/m … not measured

For 'open air' glasses, we found that the choice of the crucible material affects the fiber loss in the UV-visible range. The fibers made from glasses melted in a gold crucible show a relatively weak absorption band at 600-700 nm, while the fibers made from glasses melted in a platinum crucible demonstrate a broad and intense absorption in the UV-visible range (Fig. 2(a)). For WO_3-TeO_2 glasses melted in gold and platinum crucibles, presence of gold and platinum impurities in the glasses was determined using x-ray powder diffraction and laser ionization mass spectroscopy [38,39]. In phosphate glasses, platinum ions are known to cause broad absorption over the UV-visible range due to charge transfer and d-d transitions [40]. According to these results, we hypothesize that the UV/Vis absorption of our tellurite glasses is affected by the presence of gold and platinum species in the glasses as a result of crucible corrosion by the glass melt. Further work is in progress to determine the gold and platinum impurity levels and identify the species responsible for the UV/Vis absorption in our glasses. Note that the lower loss of fiber #3 compared with fiber #1 is attributed to the use of higher purity TeO_2; the billet of fiber#1 was made from 99.99% TeO_2, whereas the billet of fiber #3 was made from 99.999% TeO_2.

To gain insight into the impact of the crucible material when melting in dry air, we used both gold and platinum crucible for the fabrication of billets in dry air. We commenced by melting in a gold crucible. The batch of billet #4 was first melted at 900 °C for 1 h using a lid and swirling the melt four times. Then the lid was removed and the melt kept at 900 °C for 1 h before casting. The next melt (billet #5) was produced using a platinum crucible. The glass was also melted for approximately 2 h. However, due to temporary malfunction of the furnace set-up, the melting temperature for the first 1 h was only 700-800 °C and for the second melting hour the lid was not removed. The third 'dry air' melt (billet #6) was also undertaken in a platinum crucible using the same melting conditions as for the first 'dry air' melt (billet #4) undertaken in a gold crucible.

For the 'dry air' fibers #5 and #6, we evaluated the OH content of the corresponding billets and rods via measuring the OH peak loss at 3.3 µm. In both cases, the rod and

#162011 - $15.00 USD Received 23 Jan 2012; revised 1 Mar 2012; accepted 8 Mar 2012; published 16 Mar 2012

corresponding billet exhibit the same OH content within the measurement error of ± 5 dB/m. This result indicates that annealing of the rods in open air did not increase the OH content in the glass. Another noteworthy result is that for the same melting time of 2 h, billets #5 and #6 have higher OH content (90-100 dB/m) than the glass blocks presented in Section 3 (50-60 dB/m). This is attributed to the larger batch weight of the billets (100 g) compared with the glass blocks (50 g). As the same crucible was used, the larger batch weight results in a smaller surface-to-volume ratio, which makes removal of water more difficult.

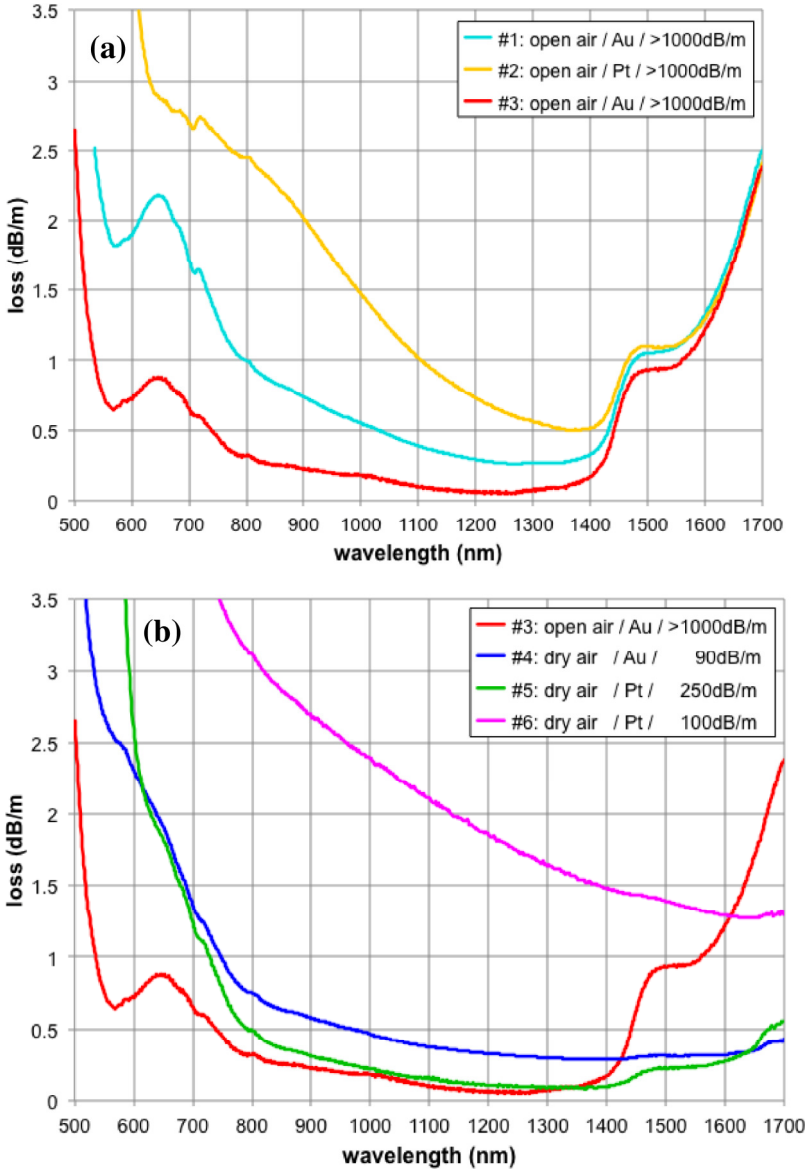

Fig. 2. Fiber loss spectra in the range 500-1700 nm for (a) 'open air' fibers #1-3 and (b) 'dry air' fibers #4-6 relative to 'open air' fiber #3. The loss numbers given in the legends refer to the loss of the OH peak at 3.3 µm of the extruded rods used for drawing the fibers.

Billet #6 and rod #4 exhibited a crack after annealing, which suggests that the procedure for annealing in dry atmosphere requires improvement. Possibly the removal of water from the glass changed the glass transition temperature (Tg) and therefore the annealing procedure needs to be modified. In the future, glass properties such as Tg, viscosity and thermal

#162011 - $15.00 USD Received 23 Jan 2012; revised 1 Mar 2012; accepted 8 Mar 2012; published 16 Mar 2012

expansion coefficients for ‘open air’ and ‘dry air’ glasses will be explored. Due to the crack in billet #6, bubbles were formed in the corresponding rod #6 during extrusion.

Figure 2(b) shows the loss of fibers #3-6 in the wavelength rage of 500-1700nm. These fibers were made using the same raw materials. As mentioned above, comparison of ‘dry air’ fibers #1 and #2 demonstrates that the use of a platinum crucible results in higher loss in the UV-visible range up to ~1400 nm. Comparison of ‘dry air’ fibers #4 and #5 that were made from glasses melted in a gold and platinum crucible, respectively, also shows additional loss in the UV-visible range <600 nm for the fiber #5 made from glass melted in a platinum crucible. However, the loss in the wavelength range 600-1400 nm is similar for both fibers. This is in contrast to ‘open air’ fibers #1 and #2. Further investigations are required to identify if the use of different raw material purity and/or the use of different melting atmosphere is the cause for the difference in loss in the 600-1400 nm wavelength range for the two fibers #2 and #4 made from glass melted in a platinum crucible.

Next we consider the loss of the ‘dry air’ fibers #4-6 relative to the ‘open air’ fibre #3 (Fig. 2(b)). ‘Dry air’ fiber #5 shows approximately the same loss at 800-1400 nm as the ‘open air’ fiber #3. ‘Dry air’ fiber #4 shows a slightly elevated loss in this wavelength region and a significantly higher loss for <700 nm relative to fiber #3. There are two possible reasons for this higher loss: firstly the crack in the corresponding rod resulted in defects in the fiber and secondly presence of gold particles in the glass. Both defects and gold particles would increase scattering loss. ‘Dry air’ fiber #6 shows considerably higher loss than both the ‘open air’ fiber #3 and ‘dry air’ fibers #4 and #5. Rod #6 contained bubbles that are considered to cause pronounced scattering loss. All three ‘dry air’ fibers #4-6 demonstrate significantly lower loss for the OH peak at 1.48 µm and at longer wavelengths. For fibers #4 and #6, the OH peak is barely visible, whereas fiber #5 shows a distinct OH peak though with significantly lower intensity relative to the ‘open air’ fiber #3. This difference in the peak intensity at 1.48 µm agrees with the variation of the OH peak intensity at 3.3µm for the rods and billets (Table 1). The higher OH content for fiber #5 relative to the other ‘dry air’ fibers is attributed to the lower melting temperature of the corresponding billet #5. As a result, the glass melt viscosity was higher, which hinders the removal of water from the melt.

To investigate the impact of melt dehydration on fiber loss at longer wavelengths, we also measured the loss for fibers #3 and #4 in the range of 1500-2400 nm (Fig. 3). Dehydration of the melt led to considerably reduced loss at longer wavelengths. For fiber #4, the loss is 0.8 dB/m at 2.0 µm and 1.7 dB/m at 2.3-2.4µm. Compare the ‘open air’ fiber #3 has an order of magnitude higher loss: 9 dB/m at 2.0 µm and ≥20 dB/m at 2.3-2.4 µm. The ten times loss reduction at 2.0-2.4 µm from ‘open air’ to ‘dry air’ fiber is consistent with the ten times loss reduction of the 3.3 µm fundamental OH absorption band. This indicates that the broad absorption between the overtone and the fundamental absorption is directly linked to the fundamental absorption at 3.3 µm.

#162011 - $15.00 USD Received 23 Jan 2012; revised 1 Mar 2012; accepted 8 Mar 2012; published 16 Mar 2012

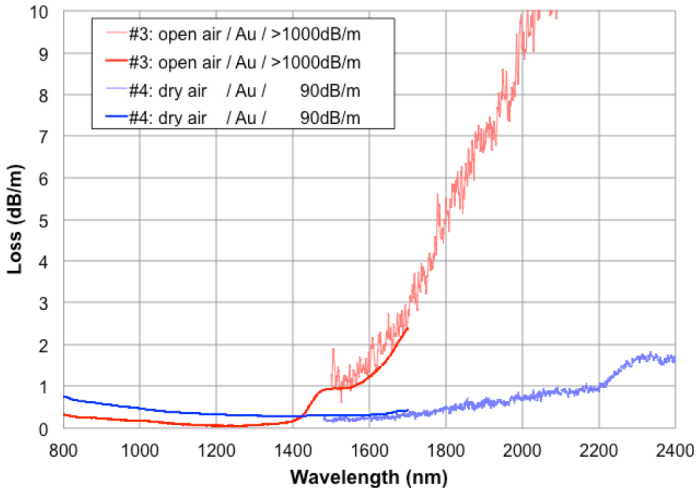

Fig. 3. Fiber loss spectra for 'open air' and 'dry air' fibers in the range of 1500-2400 nm measured using supercontinuum white light source. For comparison, the loss spectra measured up to 1700 nm using tungsten filament bulb and different OSA are also shown. The loss numbers given in the legends refer to the loss of the OH peak at 3.3 µm of the extruded rods used for drawing the fibers.

5. Conclusions

Using a dry atmosphere glass melting process, we fabricated tellurite glasses and extruded tellurite fibers with significantly reduced OH content compared to melting in open air using the same commercial raw materials and comparable melting temperatures and times. For small glass melts of 30-50 g, the use of long melting times and either frequent swirling of the glass melt or removing the crucible lid resulted in a decrease of the OH content by more than an order of magnitude. To the best of our knowledge, we achieved the lowest reported OH content in a fluoride-free tellurite glass using commercial raw materials.

We also successfully reduced the OH content in larger glass melts of 100 g. This size allows the fabrication of long fiber length (>100 m) using the extrusion technique for preform fabrication. The extruded fibers made from 'dry air' glass demonstrated significantly lower absorption for the OH vibration overtone at 1.48 µm. In addition, the lower OH content reduced the loss at wavelengths >1.5 µm by an order of magnitude compared with fibers made from 'open air' glass. We achieved fiber losses of 0.8 dB/m at 2.0 µm and 1.7 dB/m at 2.3-2.4 µm for our extruded fibers. The significant lower loss of the 'dry air' fibers for wavelength >1.5 µm opens up applications for these fibers including efficient supercontinuum generation extending into the mid-infrared. In addition, the lower loss opens up the prospect of tellurite fiber lasers that operate more efficiently in the near-infrared up to ~2.5 µm, beyond which rare earth emission is limited by multiphonon relaxation.

In the future, we will extend the fabrication of tellurite glass with reduced OH content to larger melt sizes in order to pave the way towards low-OH microstructured tellurite fibers that will demonstrate efficient lasing and supercontinuum generation in the near- to mid-infrared.

Acknowledgments

We acknowledge the DSTO (Australia) for support for the Centre of Expertise in Photonics, and the Australian Research Council for funding this project (DP0987056). We wish to thank the following associates at the University of Adelaide for their help with this research: Rachel Moore and Herbert Foo for glass fabrication, Roger Moore and Alastair Dowler for fiber fabrication, and Robin Pötter for extrusion and transmission measurements. T. Monro acknowledges the support of an Australian Research Council Federation Fellowship.

#162011 - $15.00 USD Received 23 Jan 2012; revised 1 Mar 2012; accepted 8 Mar 2012; published 16 Mar 2012